SH1D and Complex H/V Transfer Function Spatial Patterns: Central Mexico Earthquake

Marshall Pontrelli, Dr. Laurie Baise, Dr. Jonathan Lamontagne
Tufts University, Department of Civil and Environmental Engineering, Medford MA, 02155

Introduction

The magnitude 7.1 Central Mexico Earthquake occurred on 19 September 2017, killing 370 people, injuring over 6,000 and collapsing over 40 buildings. Many of these collapses and casualties took place in Mexico City, built on a historic lakebed with soft, low velocity soils overlying hard, high velocity bedrock. This structure tends to resonate, known colloquially as a location's "site effect", where local geology amplifies incoming shear waves at certain frequencies more than is expected given the source's distance. In this study we use Nakamura's (Nakamura 1989) H/V technique to compute the empirical transfer function (hereon ETF) of 58 Mexico City ground motion stations and fit to the results to the Thomson-Haskell theoretical transfer function (hereon TTF), solving for the depth to the high velocity layer, d, and the damping value, κ, using differential evolution. We categorized the results into 3 categories: SH1D, which conforms to the Thomson Haskell transfer function, complex, in which resonance frequencies are apparent but in patterns that differ from the TTF and no resonance, in which no distinct peak is apparent.

Normal incidence shear waves propagating vertically through low velocity overburden overlying high velocity basement amplify at

$$\left|{}^{v_0}/_{2v_2}\right| = {}^{\rho_2\beta_2}/_{\rho_1\beta_1} \quad (1)$$

At periods

$$T_m = \frac{4d_1}{m\beta_1} \quad (2)$$

Where

v_0 = displacement amplitude at free surface
v_2 = displacement amplitude of the 2nd layer
ρ_n = density of the nth layer
β_n = shear wave velocity of the nth layer
T = period
d_n = depth of the layer
m = harmonic # (1, 3, 5 etc.)

(Haskell 1960). Geologic basins, e.g. Boston and Mexico City, are typical high impedance (eq. 1) contrast structures which amplify free surface displacement, affecting civil structures during earthquakes. The Haskell-Thomson transfer function estimates site response at a location given the parameters ρ_1, β_1, ρ_2, β_2, d, and the damping κ, assuming one-dimensional vertical shear wave propagation. Using the program Nrattle (Boore 2005) we generate Haskell-Thomson theoretical transfer functions by varying values of ρ, d, β, and κ. We fit this model to real ground motion data from the 2017 Central Mexico Earthquake by computing the residual between theoretical and empirical transfer function and solving for least squares. The minimum solution is nontrivial, and we present tests using global optimization techniques brute force and differential evolution and the local minimum technique downhill simplex. The categorized results are mapped and their spatial structures analyzed.

Objective Function Design

We designed an objective function which fits the Thomson-Haskell theoretical transfer function to an H/V empirical transfer function using the method of least squares (eq. 3, 4).

$$r_i = y_i - f(x_i, \beta) \quad (3)$$

$$S = \sum_{i=1}^{n} r_i^2 \quad (4)$$

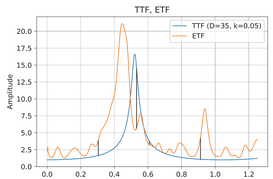

Figure 1. Demonstration of the objective function. Black lines are the residual r_i, the blue line is the TTF computed from NRATTLE and the orange line is the ETF computed from H/V analysis from Mexico City ground motion data.

In equation 3, y_i is the H/V empirical transfer function shown in orange and $f(x_i, \beta)$ is the theoretical transfer function shown in blue in figure 1. The output of the objective function is S, the sum of the squared residuals. The minimization techniques we test in this paper minimize S.

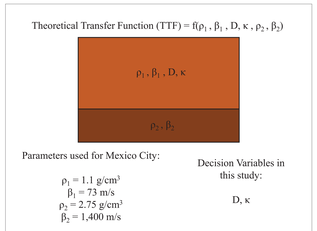

Figure 2. Graphic representation of our low velocity overburden overlying high velocity basement. The decision variables we used in this study are indicated as are the parameters.

Objective Function Sensitivity Analysis

We performed a sensitivity analysis on the objective function by varying the 6 parameters (figure 2) in the Haskell-Thomson transfer function. We used the Saltelli's sampling scheme (Saltelli 2002) with 1000 samples for a total of 14,000 function outputs and analyzed the results using a Sobol Sensitivity Analysis (Sobol 2001). Using our objective function, we fabricated a transfer function with d = 40 and κ = 0.05 to compute the residual and the sum of squares between the varying theoretical transfer functions. The bounds on the parameters were: ρ_2 (1, 1.5), β_2 (30, 100), ρ_2, (2, 2.8), β_2 (1400, 2800) and d, (10, 100). The first order Sobol indices indicate that damping has the most significant effect on the variance of the output (figure 3). Though the confidence interval is a little high, it is still within the range of values for which damping has the most influence on the system. The second order indices indicate that depth and velocity of the unconsolidated layer (Vs1) interact. We expected this from equation 2. The two properties of the basement rock Vs2 and dens2 both appear to interact with the damping but with very high error. We were not expecting this to come out of the equations and will need to be further tested (figure 4). Dens1, Vs1 and damping yielded the highest total order Sobol indices (figure 5).

Figure 3. First order Sobol index generated from 1000 Saltetti sampled points for a total of 14,000 iterations with error bars.

Figure 4. Second order Sobol index generated from the same trial with errors.

Figure 5. Total order Sobol index with errors.

Objective Function Space

We generated a TTF using depth = 40, κ = 0.05 and applied the brute force method with depth bounds (0, 100) and κ bounds (0, 0.20) to solve for the fabricated TTF parameters. The resulting contour plot (figure 6a) displays the results. bounds (0, 0.20). The minimum solution was solved but took 14:25 hours. The same analysis was done for empirical transfer functions computed by Nakamura's H/V from ground motion data during the Central Mexico Earthquake. The bounds for this experiment were depth: (30, 100) and κ: (0, .15). The plot is shown in figure 6b and strongly resembles figure 6a except the low function value band at low depths is cut out and we observed increased noise. A clear global minimum is apparent in dark blue at about (40, 0.02).

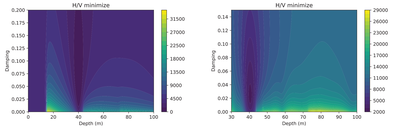

Figure 6. (a) Contour plot generated from brute force optimization with depth bounds (0, 100) and κ bounds (0, 0.20). Each axis used 100 samples for a total 10,000 iterations. (b) Contour plot generated from brute force optimization on H/V ETF with depth bounds (30, 100) and κ bounds (0, 0.15). Each axis used 100 samples for a total 10,000 iterations.

We applied the downhill simplex algorithm at a starting point (75, 0.14) and the minimization succeeded (figure 7a). Applying the same algorithm at a starting point (90, 0.14), however, failed solving for a point at (123, 0.04) (figure 7b)

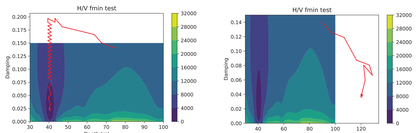

Figure 7. (a) Downhill simplex algorithm path (red line) overlying the solution space computed from the brute algorithm on H/V ETF. Starting point is at (75, 0.14) and the final point is at (40, 0.025). (b) The same algorithm but at starting point (90, 0.14) solving at a final point (120, 0.04).

We concluded that there are multiple minima in our optimization space and we had two options for minimization: pick a starting point we hope yields the correct solution or use global minimization solution techniques. We applied a differential evolution algorithm which always correctly solved for the global minimum (figure 8).

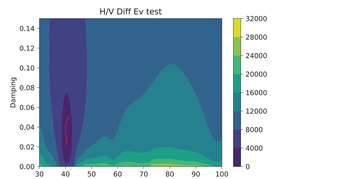

Figure 8. The path differential evolution takes to solve the same problem presented in figure 9.

The number of iterations differential evolution required for this trial was 10, function evaluations 333 and time 00:28:45. This was a manageable amount of time so we applied differential evolution to all 58 stations.

Spatial Analysis

Mexico City is divided into three geotechnical zones: Zone I (Hills), Zone II (Transition), and Zone III (Lake). We mapped the CIRES stations with their corresponding soil classification (figure 9). We included a label "compact" for sites that were indicated as such from the CIRES database. These sites, it turns out, have much different ETFs than other sites within the Lake Clay Zone. From the H/V analysis, we picked the fundamental site frequency, mapped it, and interpolated the results using ordinary kriging with a circular model: major range = 0.107, partial sill = 0.113, lag size = 12, and number of lags = 10 (figure 10).

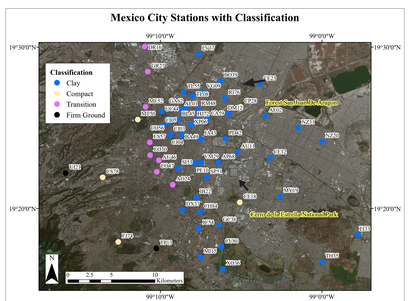

Figure 10. Adapted soil and geotechnical classifications of Mexico City from CIRES station database.

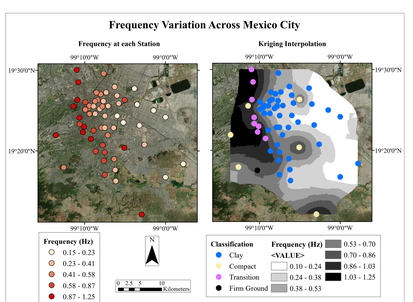

Figure 11. (a) Fundamental site frequency at each of the CIRES stations computed from the H/V analysis. (b) Ordinary kriging results of the data from (a) with a circular model: major range = 0.107, partial sill = 0.113, lag size = 12, and number of lags = 10.

We categorized the results into 3 categories: SH1D, which conforms to the Thomson Haskell transfer function, complex, in which resonance frequencies are apparent but in patterns that differ from the TTF, and no resonance, in which no distinct peak can be seen. We have provided the 6 SH1D examples with conformity to the harmonic structure, 3 examples with complex structure and 3 examples of no-resonance (figure 12).

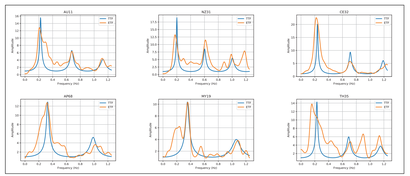

Figure 12. SH1D examples with conformity to harmonic structure, plotted in blue in figure 15.

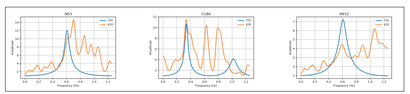

Figure 13. Examples of complex structure, plotted in violet in figure 15.

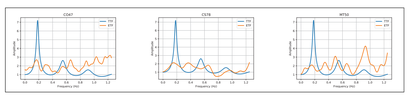

Figure 14. Examples of no resonance, plotted in red in figure 15.

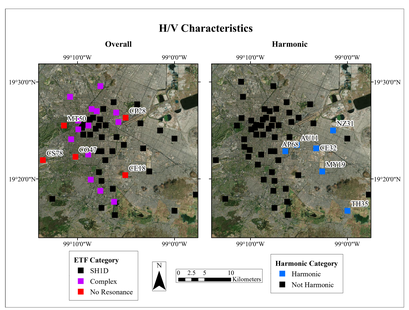

Figure 15. (a) Spatial structure of SH1D, complex (figure 13) and no distinct resonant structures (figure 14). (b) Stations displaying conformity to harmonic structure (figure 12).

Discussion

Differential evolution is the best solution to this problem because the objective function that we designed required a global minima solution. Station frequencies varied between about 0.15 Hz and 1.25 Hz so the differential evolutionary algorithm failed at higher frequencies when depth bounds could not possible reach the peak frequency (eq. 2). It therefore solved for the second harmonic matching up with the high peak. In some cases where the transfer function was either very complex or did not display resonance, the minimization failed to solve for the peak but in these cases the SH1D assumption falls apart anyway.

The three categories of results were mapped as well as the spatial distribution of the peak frequencies. There is a distinct frequency trend from low to high from east to west of the basin indicating shallower depths to the high velocity consolidated layer (figure 11). Complexity also increases from east to west (figure 15) as we move from clay lakebed sediments to the transition zone and to solid ground where SH1D assumptions fall apart. In the case of stations like CE18 (figure 12) where no resonance is displayed in the ETF, the location of the station can be correlated to a geologic feature that rises out of the lakebed, in the case of CE18, a volcano.

Conclusion

We assumed normal incidence shear waves propagating vertically through low velocity overburden overlying high velocity basement or SH1D, in Mexico City and fit the Thomson-Haskell transfer function to H/V empirical transfer functions using differential evolution. We then categorized the results into SH1D, complex or not resonant based on the correlation between TTF and ETF. We mapped the results and found that as frequency increases from east to west, so does complexity of the empirical transfer function. A distinct area of ETFs that exhibit strong SH1D characteristics is apparent on the east side of the city.

Site response is a problem in Mexico City that has caused the loss of thousands of lives. The better we understand the resonant geologic structure causing site amplification, the better prepared we will be in the future by writing site spatial characteristics into the building code of Mexico City. The objective function we designed is applicable to all structures that demonstrate SH1D and we plan on applying the presented methodology on passive microtremor data in Boston MA.

References

Boore, D. M. (2005). SMSIM-Fortran Programs for Simulating Ground Motion from Earthquakes: Version 2.3-A of OFR 96-80-A. United States Department of the Interior. U. S Geological Survey.

Campillo M., Gariel, J. C., Aki, K. Sanchez-Sesma, F.J. (1989). Destructive Strong Ground Motion in Mexico City: Source, Path, and Site Effects During Great 1985 Michoacan Earthquake Bulletin of the Seismological Society of America 79(6): 1718-1735.

Haskell, N. A. (1960). Crustal Reflection of Plane SH Waves. Geophysical Research 65(12): 4147-4150.

Nakamura, Y. (1989). A Method for Dynamic Characteristics Estimation of Subsurface using Microtremor on the Ground Surface. Railway Technical Research Institute 30(1): 25-33.

Saltelli, A. (2002). Making best use of model evaluations to compute sensitivity indices. Computer Physics Communications 145(2): 280-297.

Sobol, I. M. (2001). Global Sensitivity indices for nonlinear mathematical models and their Monte Carlo estimates. Mathematics and Computers in Simulation 55(1-3): 271-280.

Stephenson, B. Lomnitz, C. (2005). Shear-wave velocity profile at the Texcoco strong-motion array site, Valley of Mexico. Geofisca Internacional 44(1): 3-10.